Additive noise effect in digital phase detection

Yves Surrel

The characteristic polynomials associated with the algorithms used in digital phase detection are used to investigate the effects of additive noise on phase measurements. First, it is shown that a loss factor η can be associated with any algorithm. This parameter describes the influence of the algorithm on the global signal-to-noise ratio (SNR). Second, the variance of the phase error is shown to depend mainly on the global SNR. The amplitude of a modulation of this variance at twice the signal frequency depends on a single parameter β. The material presented here extends previously published results, and as many as 19 algorithms are analyzed. © 1997 Optical Society of America

1. Introduction

Most optical methods of measurement or control involving interferences or spatially periodic structures benefit a great deal from the so-called phase-shifting technique, which is referred to in Ref. 1 as phase sampling. Indeed the term phase-shifting, which is commonly used, may not be the best choice because it refers to the action of a particular device, the phase shifter, rather than to the basic feature of the measurement, which is the determination of the phase lag of a quasi-periodic signal from a set of sampled values. Although many techniques require a phase shifter, some do not. For example, the grid techniques used in displacement measurement can provide the phase-field data from one single frame when the illumination sampling frequency determined by the CCD sensor is about an integer multiple of the grid pitch. In this case, no real phase shifting is present, only a spatial sampling of a quasi-periodic signal. So, phase-shifting would probably be more appropriately referred to as digital phase detection.

The intensity sampling is always done on a regular basis, that is, M samples are taken with an equal phase spacing of $2\pi/N$ between samples. Extensive literature concerns the different errors that can be made when sampled intensities are processed to obtain the phase. Two major causes of error have been recognized:

- The real phase shift is different from the nominal one, which is frequently referred to as miscalibration.
- The intensity profile is not perfectly sinusoidal; that is, harmonics are present in the sampled signal.

An entire set of specific algorithms has been developed to minimize one or both errors. Recently, two systematic approaches have been presented to deal with algorithm design. In Ref. 2 the necessary conditions for obtaining prescribed properties of an algorithm are analyzed, and a linear system of equations must be solved to obtain the result. The method proposed in Ref. 3 is somewhat simpler because the algorithm coefficients are those of a characteristic polynomial that can be obtained from the expansion of a product of known monomials. So, with this approach the computation is reduced to a minimum.

We show that the characteristic polynomial method presented in Ref. 3 can be used to investigate systematically the effects of additive noise. First, it is shown that with every algorithm can be associated a loss factor decreasing the signal-to-noise ratio. Second, a general analytical expression is given for the variance of the phase error.

2. Characteristic Polynomials

In this section it is briefly explained how a characteristic polynomial can be associated with any algorithm and how an algorithm insensitive to harmonics and/or miscalibration to a given order can be computed from a simple product of monomials. More details can be found in Ref. 3. We denote $\delta = 2\pi/N$ the nominal phase increment and δ^* the real phase increment by

$$\delta^* = \delta(1 + \varepsilon). \tag{1}$$

The author is with the Department of Mechanical and Materials Engineering, École des Mines de St-Étienne, 158, cours Fauriel, 42023 St. Etienne Cedex, France.

Received 26 March 1996; revised manuscript received 21 May 1996.
0003-6935/97/010271-06$10.00/0
© 1997 Optical Society of America

In the digital phase detection, M sampled intensities I_k are taken with

$$I_k = A[1 + \gamma\, \mathrm{frng}(\varphi + k\delta^*)], \tag{2}$$

where A is the local intensity bias, γ is the contrast or visibility of the intensity signal, and k takes the values $0, 1, \ldots, M-1$. The function $\mathrm{frng}(\cdot)$ describes the fringe profile. It is a 2π-periodic function, and so it is expandable into a Fourier series. What is sought is the phase φ of its fundamental component.

Usually, algorithms for digital phase detection are given as the arctangent of the ratio of two linear combinations:

$$\varphi^* = \arctan\left(\frac{\sum_{k=0}^{M-1} b_k I_k}{\sum_{k=0}^{M-1} a_k I_k}\right). \tag{3}$$

Here the measured phase is denoted by φ^* to distinguish it from the actual phase φ. This phase φ^* can also be interpreted as the argument of the complex linear combination $S(\varphi)$:

$$S(\varphi) = \sum_{k=0}^{M-1} c_k I_k, \tag{4}$$

where $c_k = a_k + ib_k$. The sum $S(\varphi)$ is also expandable into a Fourier series:

$$S(\varphi) = \sum_{m=-\infty}^{\infty} \gamma_m \exp(im\varphi). \tag{5}$$

Obviously, the argument φ^* of $S(\varphi)$ is equal to $\varphi + \arg(\gamma_1)$ if $\gamma_m = 0$ for $m \neq 1$. So, this is required for an algorithm to detect the proper phase. It is shown in Ref. 3 that this can be expressed simply if one introduces the characteristic polynomial $P(x)$ having coefficients c_k:

$$P(x) = \sum_{k=0}^{M-1} c_k x^k. \tag{6}$$

With $\zeta = \exp(i\delta)$, the following rules apply:

- When $\varepsilon = 0$, the insensitivity of the algorithm to the harmonic m is obtained when ζ^m is the root of the characteristic polynomial. For $m = 0$, this insensitivity persists when $\varepsilon \neq 0$.
- When $\varepsilon \neq 0$ and $m \neq 0$, this insensitivity is preserved if ζ^m is a double root of the characteristic polynomial. More precisely, there will be no modulating term of the order of ε in the measured phase owing to the presence of the harmonic m. Improved insensitivity, when terms of higher power in ε are eliminated, requires ζ^m to be a root of higher order of the characteristic polynomial.
- The argument of $P(\zeta)$ is an offset of the measured phase φ^*.

From these rules, it is simple to obtain algorithms with prescribed properties from the expansion of the product of monomials involving the roots. All published algorithms can be analyzed from the location and multiplicity of the roots of their characteristic polynomial. For example, the classical N-bucket algorithm is obtained from the following polynomial:

$$P_N(x) = \zeta(x-1)(x-\zeta^2)(x-\zeta^3)\ldots(x-\zeta^{N-1}) \tag{7}$$

$$= \zeta\,\frac{x^N - 1}{x - \zeta} = \frac{1 - \zeta^{-N}x^N}{1 - \zeta^{-1}x} \tag{8}$$

$$= 1 + \zeta^{-1}x + \zeta^{-2}x^2 + \ldots + \zeta^{-(N-1)}x^{N-1}, \tag{9}$$

where the multiplying constant ζ ensures that $P(\zeta)$ is real so that no offset is added to the measured phase. It is proposed in Ref. 3 to call this algorithm the discrete Fourier transform (DFT) algorithm, because it computes the argument of the first coefficient of the DFT of the set of intensities $\{I_k\}$. When $\varepsilon = 0$, it is insensitive to harmonics up to $m = N - 2$.

It is practical to represent graphically the location and multiplicity of the roots of the characteristic polynomial. In Table 1 are listed most of the algorithms that have been published in recent years, with their characteristic polynomial and associated diagram, along with parameters describing their properties with respect to noise propagation, as explained in Section 3.

3. Additive Noise

In this section, the intensity signal is supposed to be a perfect sine and the sampling spacing is supposed to be perfect, that is, $\varepsilon = 0$. Each recorded intensity I_k is supposed to be affected by additional centered noise ΔI_k of variance σ^2 and is supposed not to depend on k. It is also assumed that there is a statistical independency of the noises corresponding to two different values of intensity, i.e.,

$$\langle \Delta I_k \Delta I_m \rangle = \sigma^2 \delta_{km}, \tag{10}$$

where δ_{km} is the Kronecker delta. Throughout this section, superscript * means in the presence of noise and Δ denotes the difference between values with and without asterisks:

$$S = |S| \exp(i\varphi), \tag{11a}$$

$$S^* = |S^*| \exp(i\varphi^*), \tag{11b}$$

$$S^* = S + \Delta S, \tag{11c}$$

where the dependency of $S(\varphi)$ on φ is dropped.

A. Algorithm Loss Factor

The local signal-to-noise ratio (snr) characterizing the measuring process of a single sample is defined as

$$\mathrm{snr}^2 = \frac{\langle \tilde{I}^{*2} \rangle}{\sigma^2} \approx \frac{\langle \tilde{I}^2 \rangle}{\sigma^2} = \frac{A^2\gamma^2}{2\sigma^2}, \tag{12}$$

where $\tilde{I} = A\gamma \cos\varphi$ is the modulated intensity signal. The variance of the noise present in $|S^*|$ is $r^2\sigma^2$, where

Table 1. Examples of Algorithms that can be Found in the Literature with Their Characteristic Diagram[a]

Items	M	δ	Diagram	Coefficients[b]	η	β
(1)[10,11]	3	$\frac{\pi}{2}$	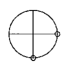	$\frac{1,\ -1,\ 0}{0,\ 1,\ -1}$ $\frac{1,\ -2,\ 1}{1,\ 0,\ -1}$	$\sqrt{\frac{2}{3}} = 0.816$	$\frac{1}{2} = 0.500$
(2)[10]	3[c]	$\frac{2\pi}{3}$	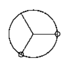	$\frac{\sqrt{3}\,[0,\ -1,\ 1]}{[2,\ -1,\ -1]}$	1	0
(3)[12–14,10,15]	4[c]	$\frac{\pi}{2}$	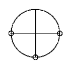	$\frac{1,\ 1,\ -1,\ -1}{-1,\ 1,\ 1,\ -1}$ $\frac{0,\ -1,\ 0,\ 1}{1,\ 0,\ -1,\ 0}$	1	0
(4)[16,15]	4	$\frac{\pi}{2}$	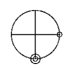	$\frac{0,\ -2,\ 2,\ 0}{1,\ -1,\ -1,\ 1}$	$\sqrt{\frac{2}{3}} = 0.816$	$\frac{1}{3} = 0.333$
(5)[17,15]	5[d]	$\frac{\pi}{2}$	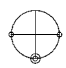	$\frac{0,\ -2,\ 0,\ 2,\ 0}{1,\ 0,\ -2,\ 0,\ 1}$	$4\sqrt{\frac{2}{35}} = 0.956$	$\frac{1}{7} = 0.143$
(6)[15,e]	5	$\frac{\pi}{2}$	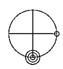	$\frac{1,\ -4,\ 0,\ 4,\ -1}{1,\ 2,\ -6,\ 2,\ 1}$	$\frac{4}{5} = 0.800$	$\frac{3}{20} = 0.150$
(7)[18]	6[f]	$\frac{\pi}{2}$	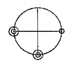	$\frac{0,\ -2,\ -2,\ 2,\ 2,\ 0}{1,\ 1,\ -2,\ -2,\ 1,\ 1}$	$\frac{4}{\sqrt{21}} = 0.873$	$\frac{1}{7} = 0.143$
(8)[15,e]	6	$\frac{\pi}{2}$	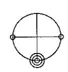	$\frac{0,\ -3,\ 0,\ 4,\ 0,\ -1}{1,\ 0,\ -4,\ 0,\ 3,\ 0}$	$4\sqrt{\frac{2}{39}} = 0.906$	0
(9)[15,e]	6	$\frac{\pi}{2}$	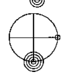	$\frac{0,\ -4,\ 4,\ 4,\ -4,\ 0}{1,\ -1,\ -6,\ 6,\ 1,\ -1}$	$\frac{8}{\sqrt{105}} = 0.781$	$\frac{3}{35} = 0.086$
(10)[2,3]	7[g]	$\frac{\pi}{2}$	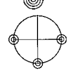	$\frac{-1,\ 0,\ 3,\ 0,\ -3,\ 0,\ 1}{0,\ -2,\ 0,\ 4,\ 0,\ -2,\ 0}$	$\frac{8}{\sqrt{77}} = 0.912$	$\frac{1}{11} = 0.091$
(11)[19]	7	$\frac{\pi}{2}$	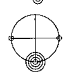	$\frac{-1,\ 0,\ 7,\ 0,\ -7,\ 0,\ 1}{0,\ -4,\ 0,\ 8,\ 0,\ -4,\ 0}$	$\frac{16}{7\sqrt{7}} = 0.864$	$\frac{1}{49} = 0.020$
(12)[20]	7[d]	$\frac{\pi}{3}$	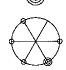	$\frac{\sqrt{3}\,[-1,\ 3,\ 3,\ 0,\ -3,\ -3,\ 1]}{3[-1,\ -1,\ 1,\ 2,\ 1,\ -1,\ -1]}$	$6\sqrt{\frac{3}{119}} = 0.953$	$\frac{2}{17} = 0.118$
(13)[20]	7	$\frac{\pi}{3}$	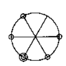	$\frac{\sqrt{3}\,[0,\ 1,\ 1,\ 0,\ -1,\ -1,\ 0]}{-1,\ -1,\ 1,\ 2,\ 1,\ -1,\ -1}$	$6\sqrt{\frac{2}{77}} = 0.967$	$\frac{1}{11} = 0.091$
(14)[19]	9	$\frac{\pi}{4}$	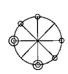	$\frac{0,\ 1,\ 2,\ 1,\ 0,\ -1,\ -2,\ -1,\ 0}{-1,\ -1,\ 0,\ 1,\ 2,\ 1,\ 0,\ -1,\ -1}$	0.970	$\frac{1}{11} = 0.091$
(15)[3]	10[f]	$\frac{\pi}{3}$	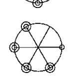	$\frac{\sqrt{3}\,[-1,\ -3,\ -3,\ 1,\ 6,\ 6,\ 1,\ -3,\ -3,\ -1]}{1,\ -1,\ -7,\ -11,\ -6,\ 6,\ 11,\ 7,\ 1,\ -1}$	$9\sqrt{\frac{2}{235}} = 0.830$	$\frac{5}{47} = 0.106$
(16)	11[g]	$\frac{\pi}{3}$	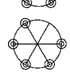	$\frac{\sqrt{3}\,[-1,\ -2,\ 0,\ 4,\ 5,\ 0,\ -5,\ -4,\ 0,\ 2,\ 1]}{1,\ -2,\ -6,\ -4,\ 5,\ 12,\ 5,\ -4,\ -6,\ -2,\ 1}$	$8\sqrt{\frac{2}{803}} = 0.898$	$\frac{4}{73} = 0.055$
(17)[2]	11	$\frac{\pi}{3}$	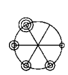	$\frac{\sqrt{3}\,[0,\ -1,\ -4,\ -7,\ -6,\ 0,\ 6,\ 7,\ 4,\ 1,\ 0]}{-2,\ -5,\ -6,\ -4,\ 8,\ 12,\ 8,\ -4,\ -6,\ -5,\ -2}$	$18\sqrt{\frac{2}{1397}} = 0.681$	$\frac{26}{127} = 0.205$
(18)[19]	11	$\frac{\pi}{2}$	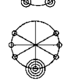	$\frac{1,\ 0,\ -8,\ 0,\ 15,\ 0,\ -15,\ 0,\ 8,\ 0,\ -1}{0,\ 4,\ 0,\ -12,\ 0,\ 16,\ 0,\ -12,\ 0,\ 4,\ 0}$	$\frac{48}{17\sqrt{11}} = 0.851$	$\frac{1}{289} = 0.003$
(19)	12	$\frac{\pi}{3}$	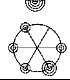	$\frac{\sqrt{3}\,[0,\ -9,\ -9,\ 9,\ 27,\ 18,\ -18,\ -27,\ -9,\ 9,\ 9,\ 0]}{2,\ 1,\ -7,\ -11,\ -1,\ 16,\ 16,\ -1,\ -11,\ -7,\ 1,\ 2}$	$\frac{\sqrt{3}}{2} = 0.866$	0

[a]For each algorithm is also given the loss factor η defined in Eq. (17) and the parameter β defined in Eq. (25a) that indicates the amplitude of the variance modulation at twice the fringe frequency, as shown in Eq. (28). There are aliased versions of these algorithms, depending on the arbitrary multiplying factor that can be placed before the characteristic polynomial. The diagrams indicate the location on the complex unit circle and the multiplicity of the roots of the corresponding characteristic polynomials.

[b]The algorithm coefficients are given in the form $b_0, b_1, \ldots, b_{M-1}/a_0, a_1, \ldots, a_{M-1}$.

[c]DFT algorithm.

[d]$(N+1)$-bucket algorithm.[21]

[e]In Ref. 15, the so-called class A algorithms have a root located at -1, and class B ones have not. This explains what is stated in the conclusion of Ref. 15, "that algorithms from class A are not sensitive to second-order detector nonlinearity" and that "the phase error caused by phase-shift miscalibration is smaller for algorithms from class B than for those from class A." In this table are listed algorithms 4A (3), 4B (4), 5A (5), 5B (6), 6A (8), and 6B (9).

[f]Minimal algorithm.[3]

[g]WDFT algorithm.

$$r^2 = \sum_{k=0}^{M-1} |c_k|^2 = \sum_{k=0}^{M-1} (a_k{}^2 + b_k{}^2). \tag{13}$$

It is easy to show from Eqs. (4) and (6) that

$$|S| = \frac{A\gamma}{2}\,|P(\zeta)|. \tag{14}$$

Hence the global signal-to-noise ratio (SNR), characterizing the whole sampling process, is

$$\mathrm{SNR}^2 = \frac{|S^*|^2}{\sigma^2 r^2} \approx \frac{|S|^2}{\sigma^2 r^2} = \frac{A^2\gamma^2}{4\sigma^2 r^2}\,|P(\zeta)|^2 = \mathrm{snr}^2\,\frac{|P(\zeta)|^2}{2r^2}, \tag{15}$$

and so

$$\mathrm{SNR} = \eta\left(\frac{M}{2}\right)^{1/2}\mathrm{snr}, \tag{16}$$

where[4]

$$\eta = \frac{|P(\zeta)|}{r\sqrt{M}} \qquad 0 < \eta \leq 1 \tag{17}$$

is a loss factor that can be associated with the characteristic polynomial, indicating how the ratio SNR/snr differs from $\sqrt{M}/2$, the optimum value that is obtained with the DFT algorithm, where the M statistically independent values I_k are combined with equal weights. In Table 1 the corresponding value of η for each algorithm is indicated. It can be seen that η is rarely less than 0.8.

B. Phase-Error Statistics

In this section, we determine the average and variance of the phase error resulting from the presence of noise.

1. *Average*

To obtain the phase-error average, we expand S^* up to the first order, starting from Eq. (11c) and using Eqs. (11a)–(11c):

$$S^* = |S|\exp(i\varphi)\left[1 + \exp(-i\varphi)\,\frac{\Delta S}{|S|}\right] \tag{18a}$$

$$= |S^*|\exp[i(\varphi + \Delta\varphi)] \tag{18b}$$

$$\approx |S^*|\exp(i\varphi)(1 + i\Delta\varphi). \tag{18c}$$

Let us denote

$$\frac{\Delta S}{|S|} = J + iK, \tag{19}$$

so that

$$J = \sum_{k=0}^{M-1} a_k\,\frac{\Delta I_k}{|S|}, \tag{20a}$$

$$K = \sum_{k=0}^{M-1} b_k\,\frac{\Delta I_k}{|S|}. \tag{20b}$$

Then Eq. (18a) can be rewritten as

$$S^* = |S|\exp(i\varphi)[1 + (\cos\varphi - i\sin\varphi)(J + iK)]$$
$$\approx |S|\exp(i\varphi)[1 + i(K\cos\varphi - J\sin\varphi)]. \tag{21}$$

So, the expression of the phase error limited to the first order is found from Eqs. (18c) and (21) to be

$$\Delta\varphi \approx K\cos\varphi - J\sin\varphi. \tag{22}$$

Hence, because $\langle J\rangle = \langle K\rangle = 0$, the average phase error cancels[5]:

$$\langle\Delta\varphi\rangle \simeq 0. \tag{23}$$

2. *Variance*

The variance of the phase error can be evaluated from approximation (22) squared and averaged:

$$\begin{aligned}\langle\Delta\varphi^2\rangle &= \langle K^2\rangle\cos^2\varphi + \langle J^2\rangle\sin^2\varphi - 2\langle JK\rangle\sin\varphi\cos\varphi \\ &= \tfrac{1}{2}[\langle J^2\rangle + \langle K^2\rangle - (\langle J^2\rangle - \langle K^2\rangle)\cos(2\varphi) \\ &\quad - 2\langle JK\rangle\sin(2\varphi)].\end{aligned} \tag{24}$$

With different notations, this expression can be found in Ref. 6. Let us define

$$\beta = \frac{\left|\sum_{k=0}^{M-1} c_k{}^2\right|}{r^2}, \tag{25a}$$

$$\theta = \tfrac{1}{2}\arg\left(\sum_{k=0}^{M-1} c_k{}^2\right), \tag{25b}$$

so that

$$\sum_{k=0}^{M-1} c_k{}^2 = \sum_{k=0}^{M-1} (a_k{}^2 - b_k{}^2 + 2ia_kb_k) = r^2\beta\exp(2i\theta). \tag{26}$$

With those definitions, we easily show, using Eq. (10), that

$$\langle J^2\rangle + \langle K^2\rangle = \frac{1}{\mathrm{SNR}^2}, \tag{27a}$$

$$\langle J^2\rangle - \langle K^2\rangle = \frac{\beta\cos(2\theta)}{\mathrm{SNR}^2}, \tag{27b}$$

$$\langle JK\rangle = \frac{\beta\sin(2\theta)}{2\mathrm{SNR}^2}. \tag{27c}$$

Using these relations, we can evaluate the phase-error variance from Eq. (24) as

$$\langle\Delta\varphi^2\rangle = \frac{1}{2\mathrm{SNR}^2}\{1 - \beta\cos[2(\varphi - \theta)]\}. \tag{28}$$

So, there is a modulation of the variance depending on the parameter β. However, it can be seen in Table 1 that β is usually much smaller than 1. In Eq. (28) results reported in Refs. 7–9 are generalized.

3. *Design of Algorithms with* $\beta = 0$

It has been shown that the variance (and also the average value[5]) of the phase error depends on the parameter β. In this subsection, it is shown how any given algorithm can be modified so that $\beta = 0$, provided an extra intensity sample is allowed.

From Eq. (26) it can be seen that the condition $\beta = 0$ is verified if and only if the sum of the squared coefficient of the characteristic polynomial is zero. Let us write the product between the characteristic polynomial associated with any given algorithm and the monomial $(x - a)$, where a is a complex number:

$$\begin{aligned} P(x)(x-a) &= \sum_{k=0}^{M} d_k x^k \\ &= (c_0 + c_1 x + \ldots + c_{M-1} x^{M-1})(x-a) \\ &= -ac_0 + (c_0 - ac_1)x + (c_1 - ac_2)x^2 + \ldots \\ &\quad + (c_{M-2} - ac_{M-1})x^{M-1} + c_{M-1}x^M. \end{aligned} \tag{29}$$

So, the sum of the squared coefficient of the resulting polynomial is

$$\sum_{k=0}^{M} {d_k}^2 = a^2 {c_0}^2 + \sum_{k=0}^{M-2} ({c_k}^2 + a^2 {c_{k+1}}^2 - 2ac_k c_{k+1}) + {c_{M-1}}^2 \tag{30}$$

$$= (1 + a^2) \sum_{k=0}^{M-1} {c_k}^2 - 2a \sum_{k=0}^{M-2} c_k c_{k+1}. \tag{31}$$

Zeroing this sum yields an equation of second degree in a, which always has a solution in the complex field. If a is taken as a root of this equation, the polynomial obtained in Eq. (29) will be the characteristic polynomial of an algorithm with $\beta = 0$, having at least the same properties as the original one as to harmonics or miscalibration insensitivity. This demonstrates how any algorithm can be modified.

Let us follow the procedure for the windowed discrete Fourier transform (WDFT) algorithm.[3] It can be found after some computations that in this case

$$\sum_{k=0}^{M-1} {c_k}^2 = \frac{N}{\sin^2(2\pi/N)}, \tag{32a}$$

$$\sum_{k=0}^{M-2} c_k c_{k+1} = \frac{N\cos(2\pi/N)}{\sin^2(2\pi/N)}. \tag{32b}$$

So, the equation to solve is written simply as

$$a^2 - 2a\cos(2\pi/N) + 1 = 0, \tag{33}$$

whose solutions are $a = \zeta^{\pm 1}$. However, $a = \zeta$ must be rejected, because this point of the complex plane acts as the detection pole for the fundamental harmonic. So, the original WDFT polynomial must be multiplied by $(x - \zeta^{-1})$.

For $N = 6$ the WDFT-algorithm coefficients are indicated in Table 1 [item (16)]. The modified algorithm is listed as item (19).

4. Conclusion

The additive noise propagation in digital phase detection has been investigated by the characteristic polynomials method. A loss factor η has been defined that describes how a given algorithm reduces the global SNR. However, for almost every known algorithm, this loss factor is not less than 0.8, as shown in Table 1. The variance in the phase error depends primarily on the global SNR, but some algorithms introduce a modulation of this variance at twice the signal frequency. The amplitude of the modulation depends on a single parameter β, and its phase lag will probably be considered not essential. However, it is demonstrated that any given algorithm can be modified to eliminate this variance modulation.

References and Notes

1. J. Schwider, "Advanced evaluation techniques in interferometry," in *Progress in Optics*, E. Wolf, ed. (Elsevier Science, New York, 1990), Vol. 28, pp. 271–359.
2. K. Hibino, B. F. Oreb, D. I. Farrant, and K. G. Larkin, "Phase-shifting for nonsinusoidal wave forms with phase-shift errors," J. Opt. Soc. Am. A **12,** 761–768 (1995).
3. Y. Surrel, "Design of algorithms for phase measurements by the use of phase-shifting," Appl. Opt. **35,** 51–60 (1996).
4. The inequalities derive from the fact that η is equal to the magnitude of the Hermitian product of the vectors $\{c_0, c_1, \ldots, c_{M-1}\}$ and $\{\zeta^0, \zeta^{-1}, \ldots, \zeta^{-(M-1)}\}$ divided by the product of their norms.
5. If the development is carried on to the second order, one finds that $\langle\Delta\varphi\rangle = (\beta/2\mathrm{SNR}^2)\sin[2(\varphi - \theta)]$. This expression corresponds to the modulation of $\langle\Delta\varphi\rangle$ mentioned in Ref. 9 and to the curves plotted therein. However, the amplitude of this modulation is much less than the standard deviation of $\Delta\varphi$, even in the worst cases of low SNR and high β. As an example, for algorithm (16) and SNR = 2, the ratio of the amplitude of the modulation of the phase-error average over its standard deviation is $\beta/\sqrt{2}\,\mathrm{SNR} = 0.07$. So, the modulation of the phase-error average is usually hidden in the phase noise.
6. C. Brophy, "Effect of intensity error correlation on the computed phase of phase-shifting interferometry," J. Opt. Soc. Am. A **7,** 537–541 (1990).
7. K. Freischlad and C. L. Koliopoulos, "Fourier description of digital phase-measuring interferometry," J. Opt. Soc. Am. A **7,** 542–551 (1990).
8. J. van Wingerden, H. J. Frankena, and C. Smorenburg, "Linear approximation for measurement errors in phase-shifting interferometry," Appl. Opt. **30,** 2718–2729 (1991).
9. C. Rathjen, "Statistical properties of phase-shift algorithms," J. Opt. Soc. Am. A **12,** 1997–2008 (1995).
10. C. L. Koliopoulos, Ph.D. dissertation (University of Arizona, Tucson, Ariz., 1981).
11. J. B. Hayes, Ph.D. dissertation (University of Arizona, Tucson, Ariz., 1984).
12. W. R. C. Rowley and J. Hamon, "Quelques mesures de dissymétrie de profils spectraux," Rev. Opt. Théor. Instrum. **42,** 519–523 (1963).
13. P. Carré, "Installation et utilisation du comparateur photoélectrique et interférentiel du Bureau International des Poids et Mesures," Metrologia **2,** 13–23 (1966).
14. J. C. Wyant, "Use of an ac heterodyne lateral shear interferometer with real time wave-front correction systems," Appl. Opt. **14,** 2622–2626 (1975).

15. J. Schmit and K. Creath, "Extended averaging technique for derivation of error-compensating algorithms in phase-shifting interferometry," Appl. Opt. **34,** 3610–3619 (1995).
16. J. Schwider, O. Falkenstörfer, H. Schreiber, A. Zöller, and N. Streibl, "New compensating four-phase algorithm for phase-shift interferometry," Opt. Eng. **32,** 1883–1885 (1993).
17. P. Hariharan, B. F. Oreb, and T. Eiju, "Digital phase-shifting interferometry: a simple error-compensating phase calculation algorithm," Appl. Opt. **26,** 2504–2506 (1987).
18. B. Zhao and Y. Surrel, "Phase shifting: six-sample self-calibrating algorithm insensitive to the second harmonic in the fringe signal," Opt. Eng. **34,** 2821–2822 (1995).
19. P. de Groot, "Derivation of algorithms for phase-shifting interferometry using the concept of data-sampling window," Appl. Opt. **34,** 4723–4730 (1995).
20. K. G. Larkin and B. F. Oreb, "Design and assessment of symmetrical phase-shifting algorithms," J. Opt. Soc. Am. A **9,** 1740–1748 (1992).
21. Y. Surrel, "Phase-stepping: a new self-calibrating algorithm," Appl. Opt. **32,** 3598–3600 (1993).